Structure, magnetic anisotropy and relaxation behavior of seven-coordinate Co(II) single-ion magnets perturbed by counteranions

Gangji Yi,[a] Chunyang Zhang,[a] Wen Zhao,[a] Huihui Cui,[b] Lei Chen,*[a] Zhenxing Wang,*[c] Xue-Tai Chen*[b] Aihua Yuan,*[a] Yuan-Zhong Liu[d,e] and Zhong-Wen Ouyang[c]

[a]*School of Environmental and Chemical Engineering, Jiangsu University of Science and Technology, Zhenjiang 212003, P. R. China, E-mail: chenlei@just.edu.cn; aihua.yuan@just.edu.cn*

[b]*State Key Laboratory of Coordination Chemistry, Nanjing National Laboratory of Microstructures, School of Chemistry and Chemical Engineering, Nanjing University, Nanjing 210093, P. R. China, E-mail: xtchen@netra.nju.edu.cn*

[c]*Wuhan National High Magnetic Field Center& School of Physics, Huazhong University of Science and Technology, Wuhan 430074, P. R. China, E-mail: zxwang@hust.edu.cn*

[d]*Suzhou Institute of Biomedical Engineering and Technology, Chinese Academy of Sciences, Suzhou, 215163, P. R. China*

[e]*Jinan Guoke Medical Technology Development Co., Ltd., Jinan 250100, P. R. China*

Electronic Supplementary Information

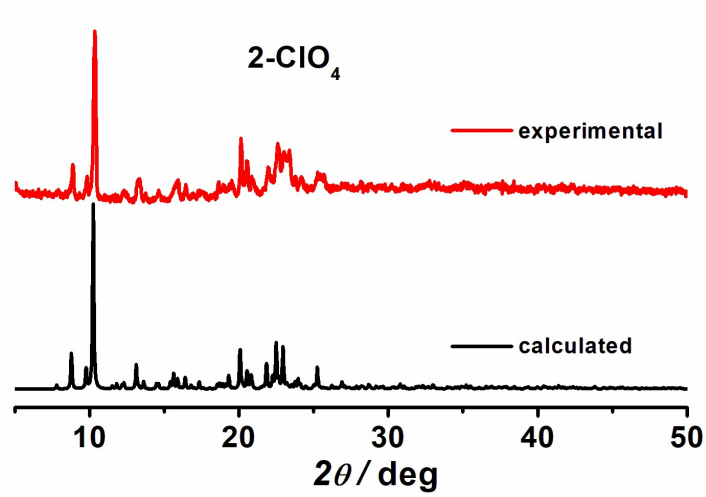

Figure S1 The powder X-ray diffraction patterns of **2-ClO$_4$** at room temperature.

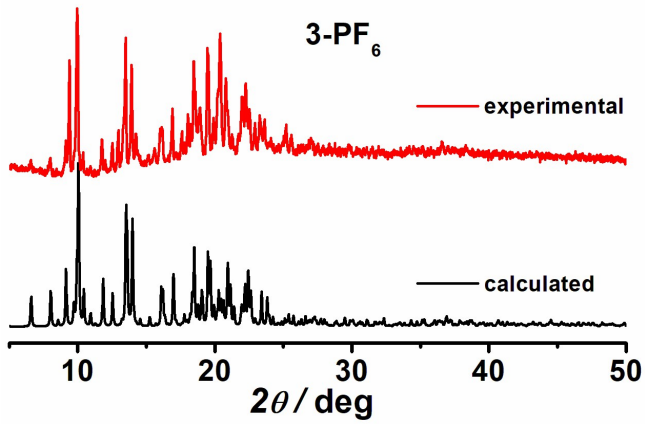

Figure S2 The powder X-ray diffraction patterns of **3-PF$_6$** at room temperature.

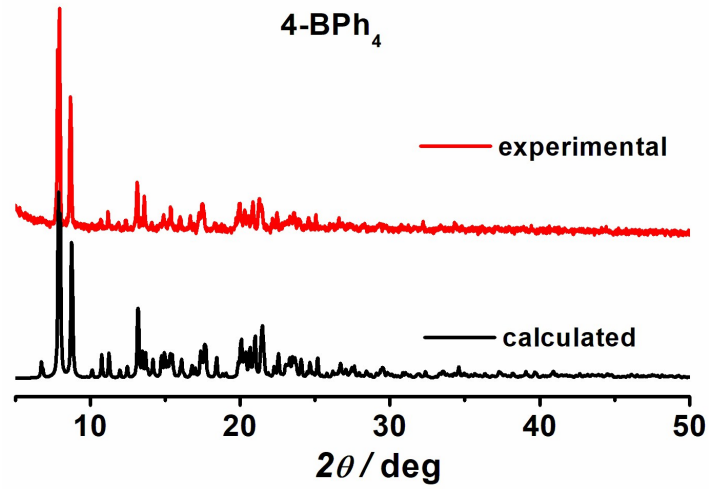

Figure S3 The powder X-ray diffraction patterns of **4-BPh$_4$** at room temperature.

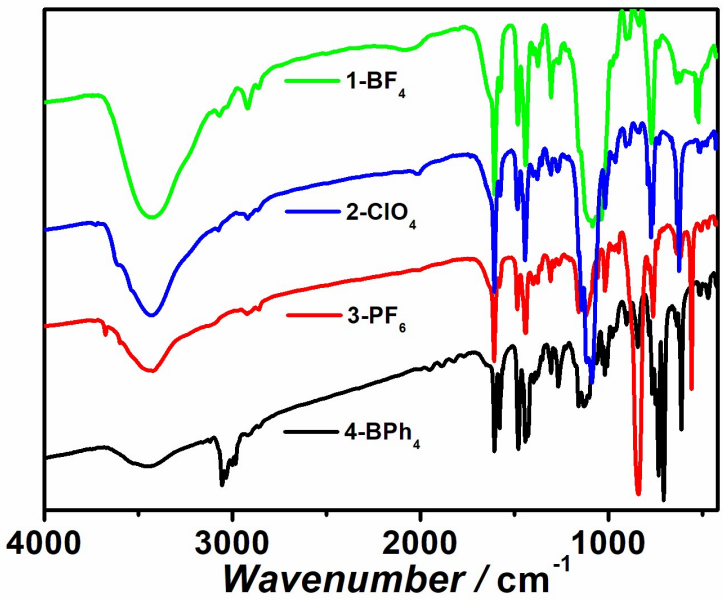

Figure S4 IR spectra for complexes **1-BF$_4$**, **2-ClO$_4$**, **3-PF$_6$** and **4-BPh$_4$**.

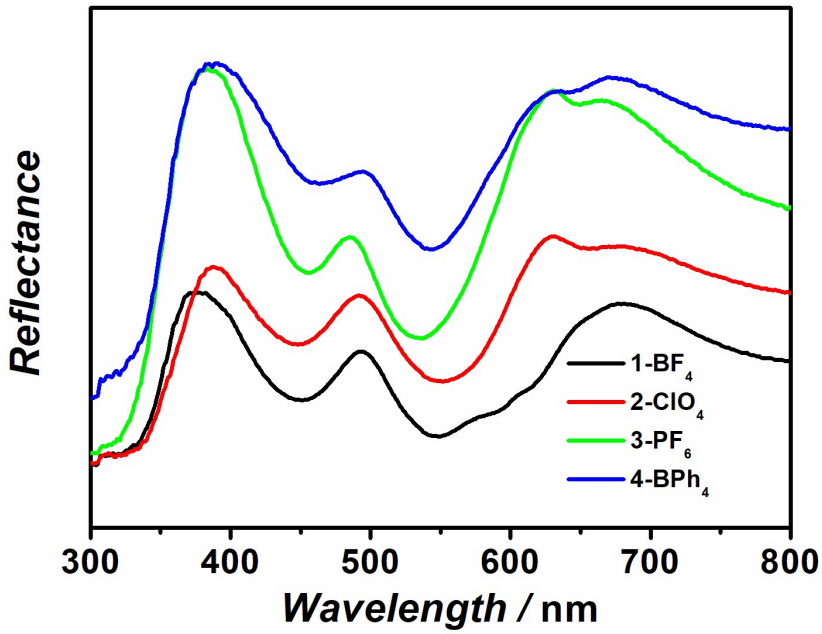

Figure S5 Solid-state diffuse reflectance spectra for **1-BF$_4$**, **2-ClO$_4$**, **3-PF$_6$** and **4-BPh$_4$**.

Table S1 Summary of crystal data and refinement for complexes **2-ClO$_4$**, **3-PF$_6$** and **4-BPh$_4$**.

	2-ClO$_4$	**3-PF$_6$**	**4-BPh$_4$**
Molecular formula	$C_{32}H_{35}Cl_2CoN_7O_9$	$C_{31}H_{31}CoF_{12}N_7P_2$	$C_{79}H_{71}B_2CoN_7$
CCDC no	1982776	1982777	1982775
Formula weight	777.47	850.50	1198.97
Temperature / K	296(2)	296(2)	296(2)
crystal system	Orthorhombic	Orthorhombic	Triclinic
Space group	*P*bca	*P*ca2$_1$	*P*-1
a / Å	18.1032(15)	20.6301(11)	13.1936(4)
b / Å	13.3310(11)	17.5943(10)	13.4238(5)
c / Å	29.071(2)	19.3260(11)	18.4168(6)
β / deg	90	90	94.625(2)
V / Å^3	7015.9(10)	7014.8(7)	3200.92(19)
Z	8	8	2
D_{calc}, g/cm^3	1.472	1.611	1.244
μ / mm^{-1}	0.704	0.680	0.319
F (000)	3208	3448	1262
Goodness-of-fit on F^2	1.032	1.104	1.003
Final R indices [$I > 2\sigma(I)$]	R_1 = 0.0653, wR_2 = 0.1270	R_1 = 0.0545, wR_2 = 0.1411	R_1 = 0.0454, wR_2 = 0.1082
R indices (all data)	R_1 = 0.1475, wR_2 = 0.1534	R_1 = 0.0800, wR_2 = 0.1592	R_1 = 0.1032, wR_2 = 0.1446

[a]$wR_2 = [\Sigma[w(F_o^2-F_c^2)^2]/\Sigma[w(Fo^2)^2]]^{1/2}$, $R_1 = \Sigma||F_o|-|F_c||/\Sigma|F_o|$.

Table S2 The results of the continuous shape measure (CShM) analyses for complexes **2-ClO$_4$**, **3-PF$_6$** and **4-BPh$_4$** by SHAPE software.[S1]

CShM	**2-ClO$_4$**	**3-PF$_6$**		**4-BPh$_4$**
		Co1	Co2	
Heptagon (D_{7h})	34.492	36.356	34.974	32.608
Hexagonal pyramid (C_{6v})	16.212	16.407	15.590	16.960
Pentagonal bipyramid (D_{5h})	5.144	6.999	7.726	3.949
Capped octahedron (C_{3v})	2.969	2.232	2.589	3.680
Capped trigonal prism (C_{2v})	2.538	2.26	3.167	2.752

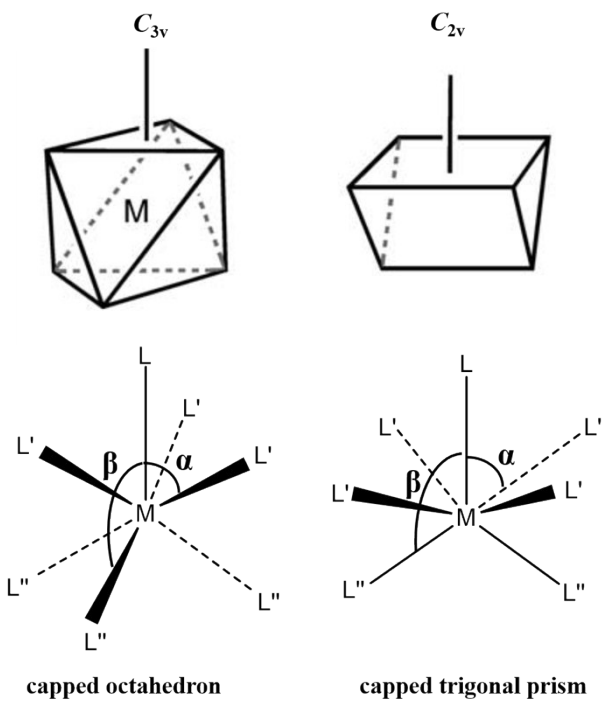

Figure S6 The structural features for two ideal polyhedrons.

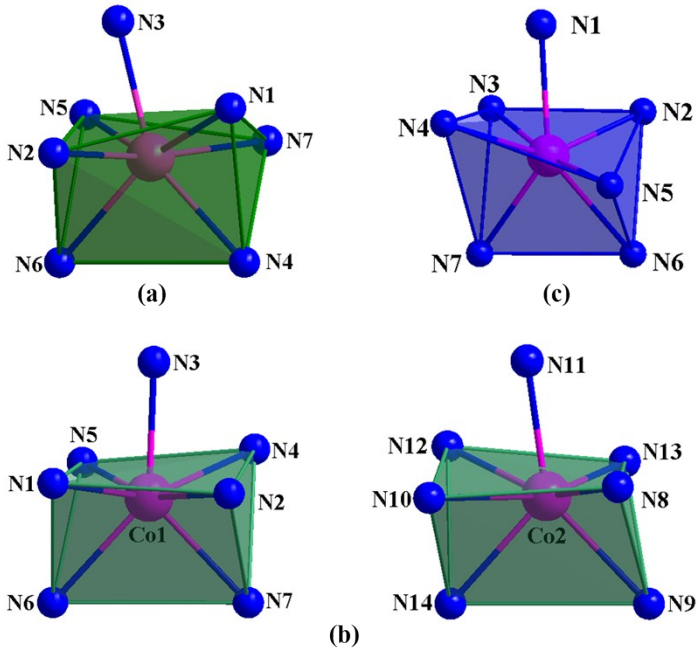

Figure S7 The coordination model of the central Co(II) ion for **2-ClO$_4$** (a), **3-PF$_6$** (b) and **4-BPh$_4$** (c).

Table S3 Selected bond lengths (Å) and angles (°) for complexes **2-ClO$_4$**, **3-PF$_6$** and **4-BPh$_4$**.

2-ClO$_4$		**3-PF$_6$**				**4-BPh$_4$**	
		Co1		Co2			
Co1-N1	2.288(4)	Co1-N1	2.261(5)	Co2-N8	2.267(5)	Co1-N1	2.287(2)
Co1-N2	2.305(5)	Co1-N3	2.100(5)	Co2-N9	2.212(5)	Co1-N2	2.138(2)
Co1-N3	2.132(5)	Co1-N4	2.258(5)	Co2-N11	2.099(5)	Co1-N3	2.406(2)
Co1-N4	2.198(5)	Co1-N5	2.298(5)	Co2-N12	2.252(5)	Co1-N5	2.242(2)
Co1-N5	2.303(5)	Co1-N6	2.181(5)	Co2-N13	2.237(6)	Co1-N6	2.305(2)
Co1-N6	2.184(5)	Co1-N7	2.201(5)	Co2-N14	2.156(5)	Co1-N7	2.140(2)
Co1-N7	**2.525(6)**	**Co1-N2**	**2.505(6)**	**Co2-N10**	**2.805(7)**	**Co1-N4**	**2.423(2)**
N3-Co1-N2	76.94(16)	N3-Co1-N1	77.2(2)	N11-Co2-N8	77.49(19)	N1-Co1-N2	75.00(8)
N3-Co1-N1	75.64(17)	N3-Co1-N2	77.54(19)	N11-Co2-N10	74.1(2)	N1-Co1-N3	74.27(8)
N3-Co1-N5	71.79(16)	N3-Co1-N4	77.4(2)	N11-Co2-N12	76.6(2)	N1-Co1-N4	70.53(8)
N3-Co1-N7	96.33(18)	N3-Co1-N5	87.91(19)	N11-Co2-N13	93.4(2)	N1-Co1-N5	99.58(8)
N3-Co1-N6	125.66(18)	N3-Co1-N6	139.8(2)	N11-Co2-N9	142.1(2)	N1-Co1-N6	142.24(8)
N3-Co1-N4	147.25(19)	N3-Co1-N7	133.9(2)	N11-Co2-N14	130.2(2)	N1-Co1-N7	141.46(8)

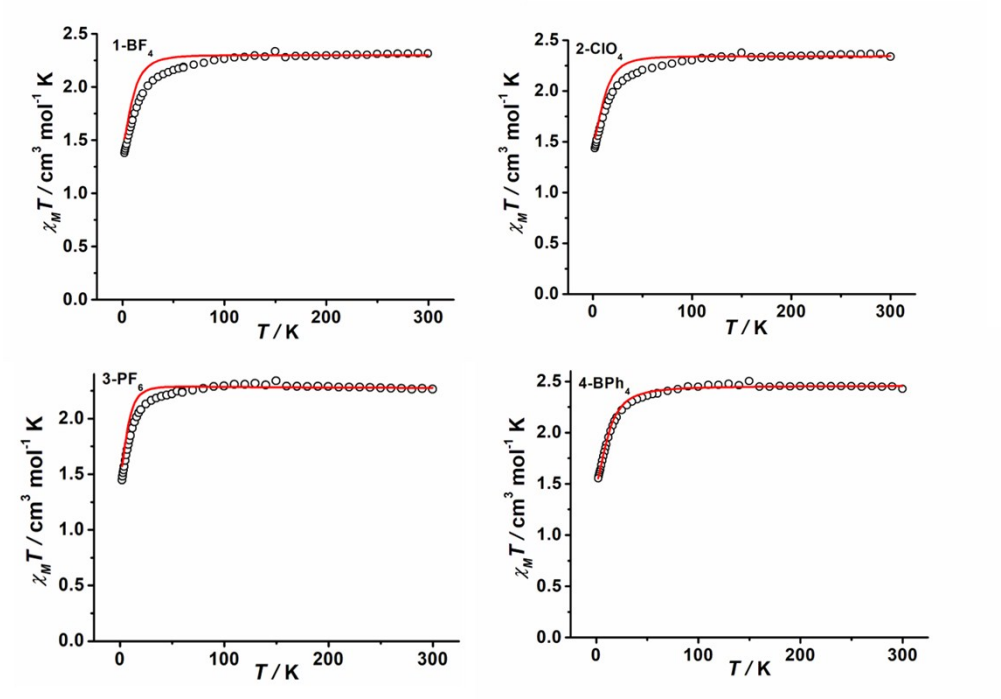

Figure S8 Variable-temperature dc susceptibility data. Solid lines indicate the best fits obtained with the PHI program.

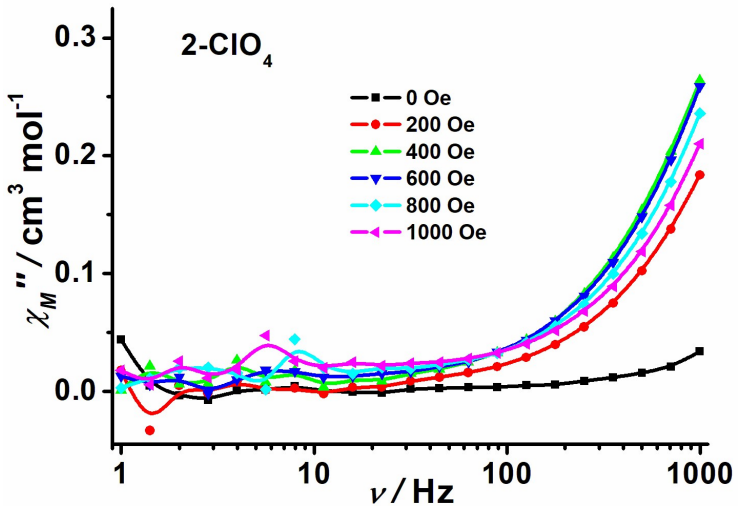

Figure S9 Frequency dependence of the out-of-phase (χ_M") ac susceptibility at 1.8 K under the applied dc fields from 0 to 1.0 KOe for **2-ClO$_4$**.

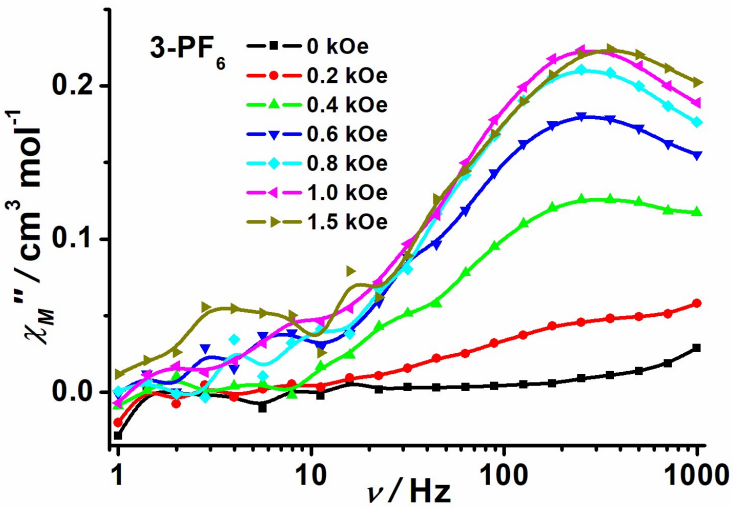

Figure S10 Frequency dependence of the out-of-phase (χ_M") ac susceptibility at 1.8 K under the applied dc fields from 0 to 1.5 KOe for **3-PF$_6$**.

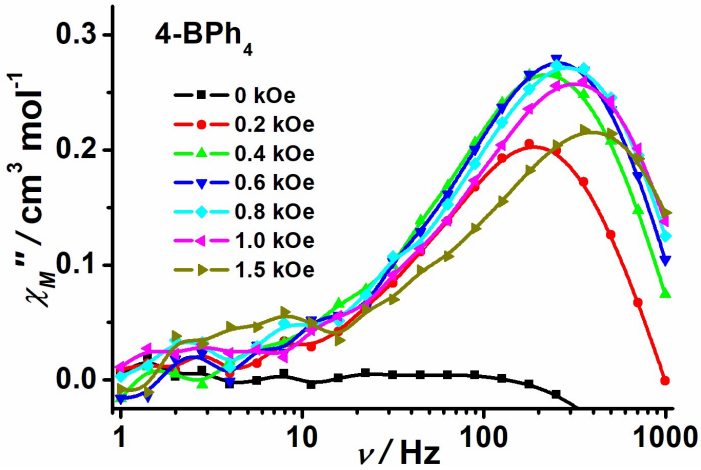

Figure S11 Frequency dependence of the out-of-phase (χ_M") ac susceptibility at 1.8 K under the applied dc fields from 0 to 1.5 KOe for **4-BPh$_4$**.

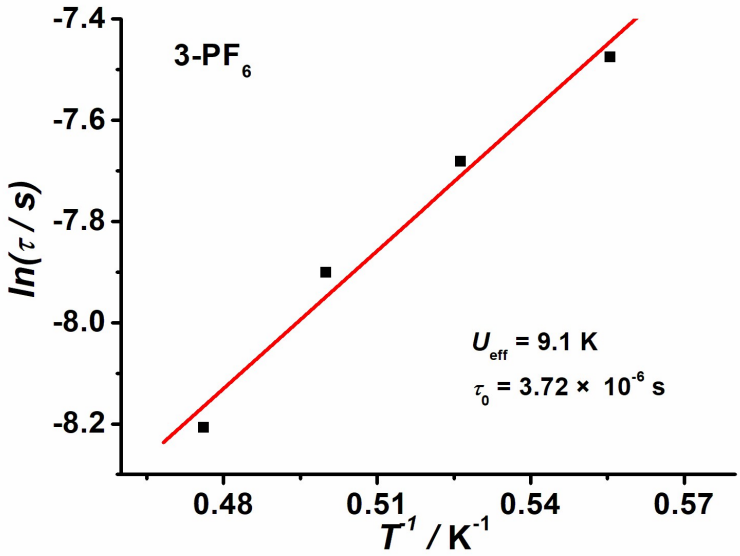

Figure S12 Relaxation time of the magnetization *ln(τ)* vs T^{-1} plot under the 1.0 KOe applied field for **3-PF$_6$**.

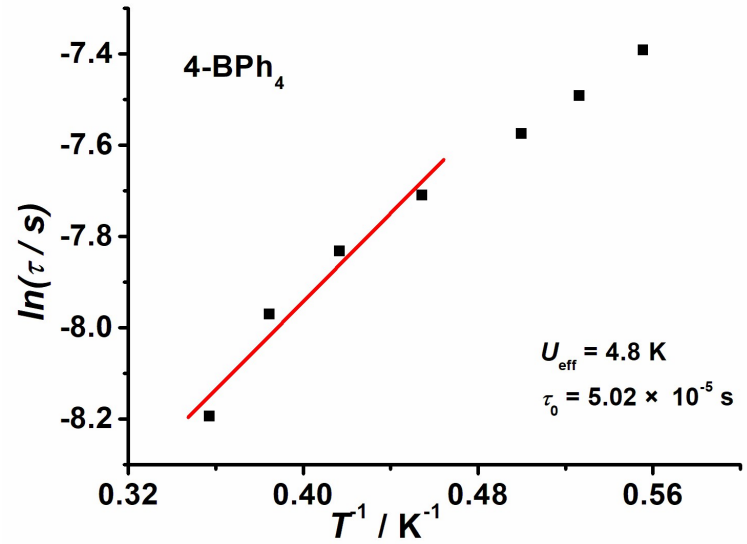

Figure S13 Relaxation time of the magnetization *ln(τ)* vs T^{-1} plot under the 0.6 KOe applied field for **4-BPh$_4$**.

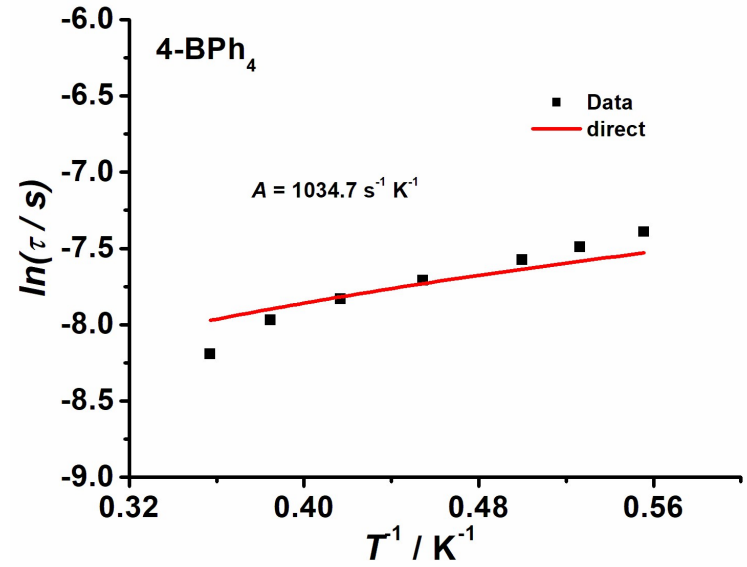

Figure S14 Relaxation time of the magnetization *ln(τ)* vs T^{-1} plot under the 0.6 KOe applied field for **4-BPh$_4$**. The red line represents the curve obtained from the fitting with the direct term.

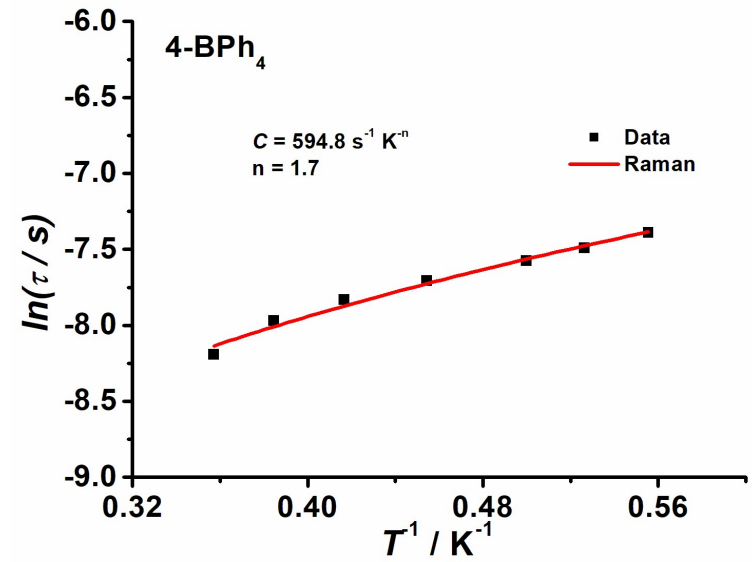

Figure S15 Relaxation time of the magnetization *ln(τ)* vs T^{-1} plot under the 0.6 KOe applied field for **4-BPh$_4$**. The red line represents the curve obtained from the fitting with the Raman term.

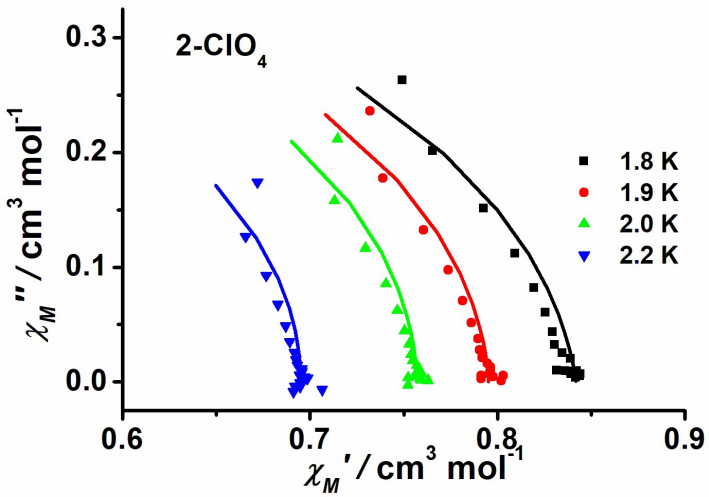

Figure S16 Cole-Cole plot obtained from the ac susceptibility data under a 0.4 KOe dc field in the temperature range of 1.8-2.2 K for **2-ClO$_4$** (solid lines represent the best fits to a generalized Debye model).

Table S4 The parameters obtained by fitting Cole-Cole plot for **2-ClO$_4$**.

T / K	χ_S	χ_T	τ	a
1.8	~0	0.842	0.0000549	0.06
1.9	~0	0.795	0.0000516	0.03
2.0	~0	0.757	0.0000482	0.01
2.2	~0	0.695	0.0000420	~0

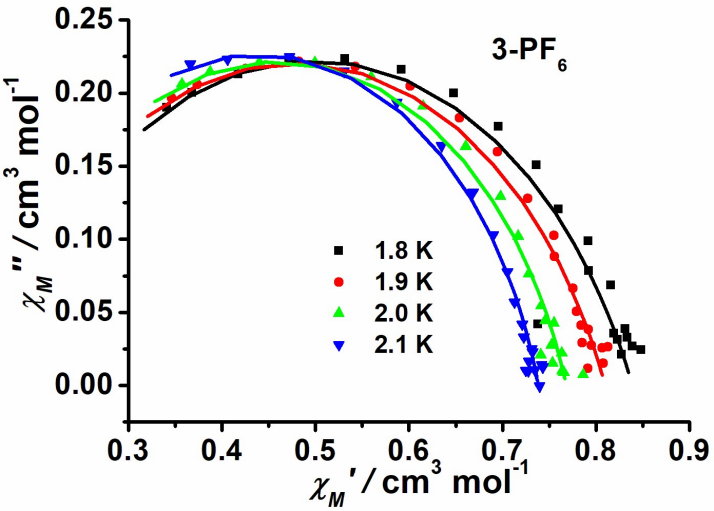

Figure S17 Cole-Cole plot obtained from the ac susceptibility data under a 1.0 KOe dc field in the temperature range of 1.8-2.1 K for **3-PF$_6$** (solid lines represent the best fits to a generalized Debye model).

Table S5 The parameters obtained by fitting Cole-Cole plot for **3-PF$_6$**.

T / K	χ_S	χ_T	τ	a
1.8	0.157	0.839	0.000502	0.26
1.9	0.147	0.809	0.000420	0.25
2.0	0.150	0.768	0.000341	0.20
2.1	0.139	0.738	0.000262	0.17

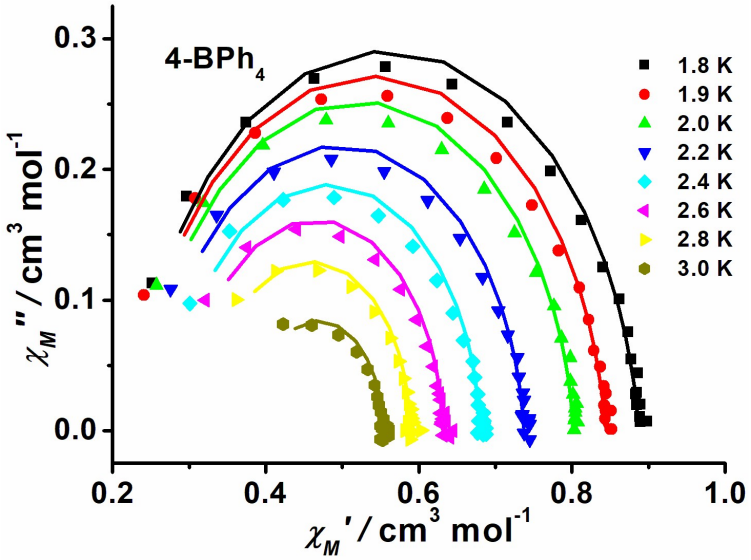

Figure S18 Cole-Cole plot obtained from the ac susceptibility data under a 0.6 KOe dc field in the temperature range of 1.8-3.0 K for **4-BPh$_4$** (solid lines represent the best fits to a generalized Debye model).

Table S6 The parameters obtained by fitting Cole-Cole plot for **4-BPh$_4$**.

T / K	χ_S	χ_T	τ	a
1.8	0.229	0.887	0.000675	0.08
1.9	0.234	0.843	0.000621	0.07
2.0	0.243	0.802	0.000572	0.07
2.2	0.258	0.737	0.000504	0.06
2.4	0.283	0.679	0.000455	0.03
2.6	0.300	0.631	0.000386	0.02
2.8	0.329	0.588	0.000304	□0

3.0	0385	0.553	0.000234	□0